

All-Optical Humidity Sensor Using SnO₂ Nanoparticle Drop Coated on Straight Channel Optical Waveguide

Nur Abdillah SIDDIQ^{1*}, Wu Yi CHONG², Yono Hadi PRAMONO¹,
Melania Suweni MUNTINI¹, Asnawi ASNAWI^{1,3}, and Harith AHMAD^{2,4}

¹Department of Physics, Institut Teknologi Sepuluh Nopember, Surabaya 60111, Indonesia

²Photonics Research Centre, University of Malaya, Kuala Lumpur 50603, Malaysia

³Department of Physics, Surabaya State University, Surabaya 60231, Indonesia

⁴Department of Physics, Faculty of Science and Technology, Airlangga University, Surabaya 60115, Indonesia

*Corresponding author: Nur Abdillah SIDDIQ E-mail: siddiq16@mhs.physics.its.ac.id

Abstract: The straight channel optical waveguide coated with the SnO₂ nanoparticle is studied as an all-optical humidity sensor. The proposed sensor shows that the transmission loss of the waveguide increases with increasing relative humidity (RH) from 56% to 90% with very good repeatability. The sensitivity to changes in relative humidity is ~2 dB/% RH. The response time of the humidity sensor is 2.5 s, and the recovery time is 3.5 s. The response to humidity can be divided into 3 different regions, which are correlated to the degree of water adsorption in the SnO₂ nanoparticle layer. Compared with the previous all-optical humidity sensor based on SnO₂, the proposed sensor exhibits more rapid response, simpler fabrication process, and higher sensitivity. The proposed sensor has a potential application in the long distance, remote agriculture, and biological humidity sensing.

Keywords: Humidity measurement; SnO₂ nanoparticle; optical sensors

Citation: Nur Abdillah SIDDIQ, Wu Yi CHONG, Yono Hadi PRAMONO, Melania Suweni MUNTINI, Asnawi ASNAWI, and Harith AHMAD, "All-Optical Humidity Sensor Using SnO₂ Nanoparticle Drop Coated on Straight Channel Optical Waveguide," *Photonic Sensors*, 2020, 10(2): 123–133.

1. Introduction

Aside from temperature, relative humidity (RH) is one of the most frequently measured physical quantities in advance applications such as material processing and manufacturing [1, 2]. Recently, a number of humidity sensors with response time of less than 1 s have been developed. These sensors can be categorized into electrical, acoustic, and optical systems. Among these sensors, the fastest response time to humidity changes is 3 ms, demonstrated in an optical system [3], compared with 8 ms in the electrical system [4] and 1 s in the acoustical system

[5]. Besides exhibiting the fastest response time, all-optical humidity sensors also have advantages such as immunity to electromagnetic interference and nuclear radiation (for high-energy physics application), water and corrosion resistance, and ability to operate in low temperature environment. Fiber-based optical sensors also allow long-range transmission of optical signals with very low loss, enabling sensor probes to be deployed in remote areas [6, 7].

The main parameter that dictates the humidity sensor performance is the rate of change in a material property to the change in the surrounding

Received: 10 January 2019 / Revised: 3 May 2019

© The Author(s) 2019. This article is published with open access at Springerlink.com

DOI: 10.1007/s13320-019-0563-8

Article type: Regular

relative humidity. Among various materials for humidity sensors, metal oxides nanoparticles have attracted special interest due to their high surface contact area with water molecules, controllable porosity, nano-sized grains, low cost, and simple construction [8–11]. Tin (IV) oxide or SnO₂ (an n-type semiconductor) is one of the useful and popular materials for humidity sensing from metal oxide group and offers a potential for developing portable and inexpensive humidity sensing device [12]. Besides that, the reason why SnO₂ is broadly used in the humidity sensor research is that it possesses many unique optical and electrical properties like wide band gap ($E_g = 3.6\text{ eV}$ at 300K), remarkable receptivity variation in the gaseous environment, high optical transparency in the visible range (up to 97%), low resistivity, and excellent chemical stability [13]. Various nanostructures of SnO₂ like nanowire and nanofiber [12, 13] have been studied as the humidity sensor based on the interdigitated electrode configuration. The performance of the SnO₂ nanostructure is remarkably superior as the humidity sensor, but there is some drawback in developing these sensors in the electronic system such as the complexity of fabrication, the use of gold (Au) as an electrode that will increase the fabrication cost, and the signals generated are prone to electromagnetic interference.

Using SnO₂ as a sensing material for all-optical humidity sensing has been reported in [14] based on a planar slab optical waveguide and in [7, 15] based on the optical fibers. The range of relative humidity measured by the planar slab optical waveguide based sensor (3%RH – 98%RH) is broader than the values reported by the optical fiber based sensors (20%RH – 90%RH). In this paper, we report an all-optical humidity sensor in the form of the SnO₂ nanoparticle layer coated on a planar stripe optical waveguide. SnO₂ nanoparticle layer coating is achieved by using the simple drop coating technique, which is a simple and effective method to fabricate the humidity sensor [4, 16]. The major improvement

introduced in the present research is the simple coating method of the SnO₂ nanomaterial onto a planar optical waveguide. The proposed all-optical humidity sensor responds to the relative humidity change between 56% RH and 90% RH with a sensitivity of $\sim 2\text{ dB}/\%\text{RH}$, a very good repeatability, and a response time.

The range of relative humidity response is broader than that of other optical humidity sensors such as the microfiber tapered-based humidity sensor using the ZnO nanoparticle layer (50%RH – 70%RH) [17] and the microfiber coupler-based humidity sensor using polyethylene oxide (70%RH – 85%RH) [18]. The sensitivity is also higher than that of the microfiber humidity sensor using ZnO nanorods (0.5221 dB/% RH) [19]. Therefore, all optical humidity sensors based on the SnO₂ nanoparticles have a potential for being used in high-energy physics applications and long-distance humidity sensing that require the fast response time.

2. Device fabrication and experiment

A silicon wafer with 7 μm of thermal oxide (TO_x) layer was used as the substrate and undercladding layer for the optical waveguide. Germanium and boron codoped silica layer were then deposited onto the substrate as a core layer. The core layer was patterned by using photolithography and etched by using inductively coupled plasma (ICP) etching followed by spin coating of ZPU13 polymer (ChemOptics, Korea) as the overcladding. To enable exposure of the propagating light field in the core to the surrounding, the ZPU13 polymer coating was etched by using oxygen plasma etching down to the top surface of the waveguide core.

Meanwhile, SnO₂ solution was prepared by dissolving 200 mg of SnO₂ nanopowder (Sigma Aldrich) with 20 ml of deionized (DI) water to obtain 1 wt% of solution concentration. The mixture was then ultrasonicated for 1 hour at the room temperature to homogeneously disperse the nanopowder. A drop of 0.5 μL SnO₂ solution was

applied onto the waveguide and then allowed to dry under the ambient condition. The time taken for the SnO₂ droplet to dry in the ambient environment is approximately 8 minutes. Drop coating of the SnO₂ layer was demonstrated in [20], which produced a room temperature gas sensor. But instead of using large droplet volume of >5 μL, multiple-drop-coating of smaller droplet volume (0.5 μL for three times) was used in this work to produce a SnO₂ nanoparticle layer with a smaller coverage area, preventing cracking of the film and increasing the adhesion between the sensing film and the planar waveguide. In addition, the multiple-drop-coating technique was also reported in [16] in coating graphene oxide layer on optical waveguides to achieve humidity sensing.

To create a controlled relative humidity environment, a homemade humidity box with controlled relative humidity between 20% RH and 90% RH was set up as depicted in Fig. 1. Two analogue mass flow controllers (MFC) were used to control the flow rate of nitrogen gas. To increase the relative humidity in the box, nitrogen gas was mixed in the mixing chamber containing deionized water to produce humid air. Meanwhile, to decrease the humidity, dry nitrogen was introduced directly to the box. A hygrometer (HI 8562 Hanna Instruments) was used to calibrate the relative humidity in the humidity box.

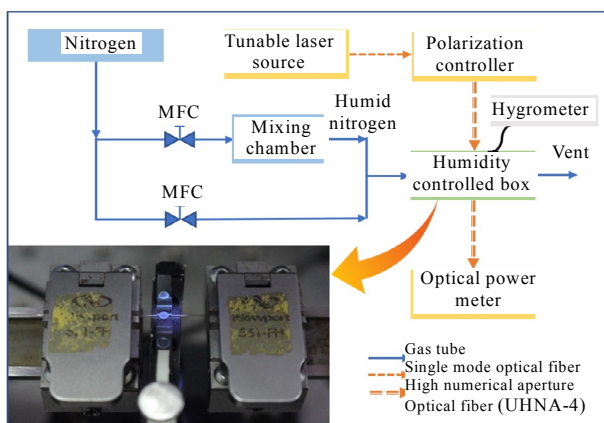


Fig. 1 Schematic diagram of the humidity sensing measurement system (inset) with the SnO₂ nanoparticle coated on the straight channel optical waveguide.

The fiber butt-coupling technique was used for light coupling with the SnO₂ coated waveguide. The optical source was a C-band tunable laser source (ANDO 4321). It was connected to a fiber polarization controller (PC) by using a standard single-mode optical fiber patch cord. The polarization controller output was connected to a standard fiber pigtail, with the other end fusion spliced to high numerical aperture optical fiber (Nufern UNHA-4) to achieve a better mode matched with the SnO₂ coated waveguide. A pair of 5-axis fiber alignment stages (Newport M-562-XYZ) were used to obtain the maximum coupling between the fibers and the waveguide as shown in the inset of Fig. 1. The transmitted power was measured by using an optical power meter (THORLABS S144C). Care was taken to keep the fiber to waveguide connection unaffected during measurement. The PC was adjusted to obtain the highest optical transmittance through the SnO₂ coated waveguide. In this case, The TM polarization was used, which showed a higher optical transmission than TE polarization.

3. Results and discussion

3.1 Characterizations of SnO₂ nanoparticles

The X-ray diffraction (XRD) pattern and scanning electron microscope (SEM) image of SnO₂ nanoparticles are shown in Fig. 2. Based on the XRD result depicted in Fig. 2(a), all reflection peaks of SnO₂ nanoparticles match well with the diffraction pattern of the tetragonal rutile SnO₂ structure (JCPDS Card No 41-1445). Impurity peaks are not observed in the XRD pattern, which means the SnO₂ nanoparticles are pure and have only the tetragonal rutile structure. The crystallite size can be estimated by using the Debye-Scherrer formula $D = k\lambda / (\beta \cos\theta)$ [10], where $k = 0.94$ is the shape factor, $\lambda = 0.1541874$ nm is the Cu-K α wavelength, and $\beta = 0.1$ rad is the full width at half maximum of the peak. The highest intensity peak, centered at $2\theta = 26.65^\circ$,

can be assigned to SnO₂ [110] reflection having d -spacing of 3.3447 Å, and the crystallite size (D) is 27.08 nm. Meanwhile, the SEM image of SnO₂ as shown in Fig. 2(b) indicates that the grain size of SnO₂ is larger than the crystallite size calculated with the XRD pattern. We believe that the agglomeration of SnO₂ nanoparticles took place, which resulted in a larger SnO₂ grain [21].

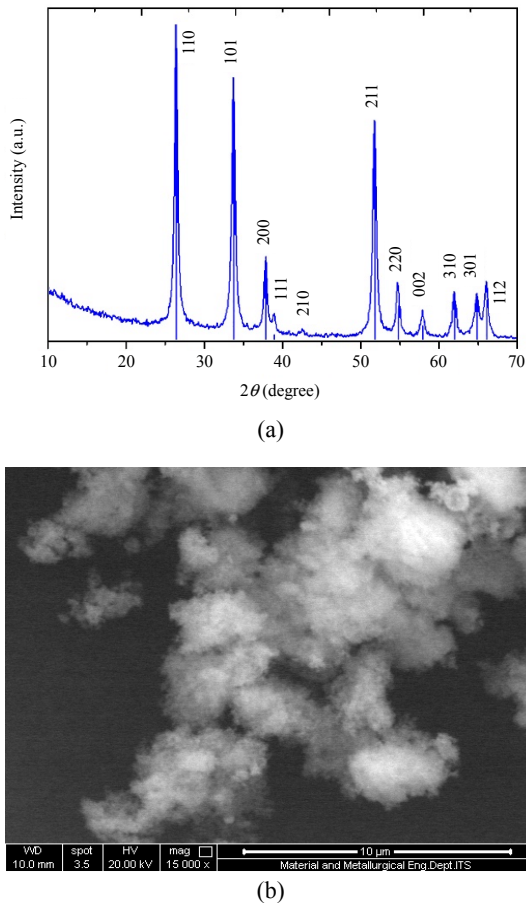


Fig. 2 Characterization of SnO₂ nanoparticles: (a) XRD pattern of SnO₂, indicating that the nanoparticles are tetragonal rutile shaped and (b) SEM images of SnO₂ nanoparticles.

3.2 Humidity sensing test

The structure of the fabricated waveguide is shown in Fig. 3(a). Both the height and width of the waveguide core were 3 μm. Then, the microscope image of the drop coated SnO₂ layer on the optical waveguide is depicted in Fig. 3(b). The coffee ring effect during the drying process can be clearly seen, which is attributed to the symmetrical dimension of

the SnO₂ nanoparticles. The insertion loss of uncoated straight waveguide was 12.7 dB. After coating with 3 drops of SnO₂, the insertion loss increased from 2 dB to 14.7 dB. The resulting SnO₂ coating with 0.5 μL SnO₂ solution had a diameter of 1.4 mm, and its average thickness was measured by using a Dektak D150 surface profiler and found to be about 2.27 μm as shown in Fig. 4(a). The effect of drop coating volume to average thickness and diameter of the resulting SnO₂ coating is depicted in Fig. 4(b). It can be seen that an increase in the droplet volume will increase the thickness and diameter from 1.82 μm to 8.2 μm and 1.2 mm to 2.2 mm, respectively.

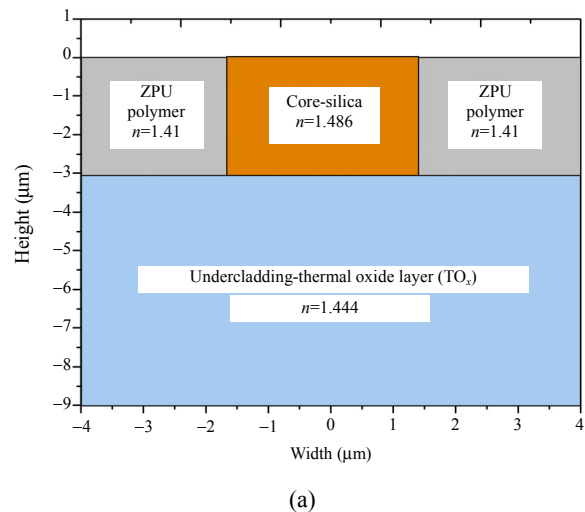
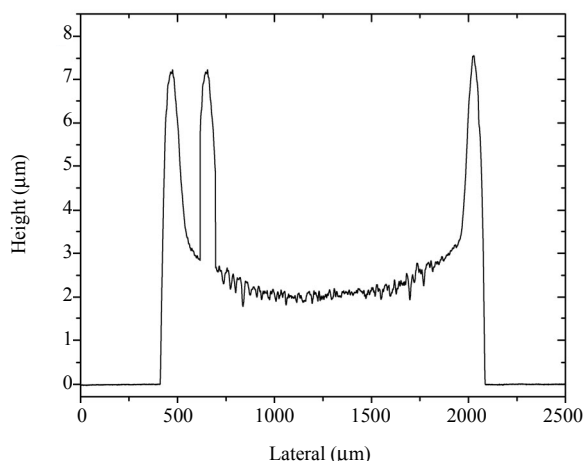
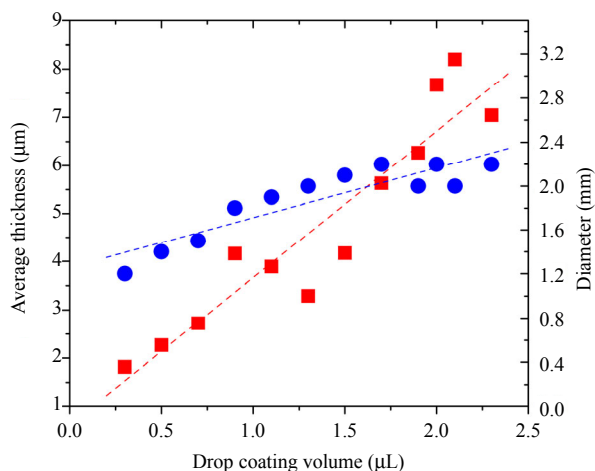


Fig. 3 Proposed device as a humidity sensor: (a) cross section of the proposed device before coating with SnO₂ nanoparticle and (b) photo of drop coated SnO₂ in the top of optical channel waveguide.



(a)



(b)

Fig. 4 SnO₂ film: (a) surface profile obtained from Dektak D150 with drop coating volume of 0.5 μL and (b) effect of drop coating volume to the average thickness and diameter of SnO₂ coating at three times drop process.

For a clearer interpretation of proposed sensor response to humidity changes, optical attenuation was used instead of the measured transmitted power. The optical attenuation (*Loss*) is defined as

$$Loss = P_{init} - P_{RH} \quad (1)$$

where P_{init} and P_{RH} are transmitted power in the initial condition (ambient condition) and transmitted power at a certain value of relative humidity, respectively.

Figure 5 shows the change in the optical attenuation when the humidity was increased from 20% RH to 90% RH. The optical attenuation increased, corresponding to a decrease in the

transmitted power through the SnO₂ coated waveguide, when the relative humidity was increased. The magnitude of optical attenuation also increased with an increase in the relative humidity, indicating that this response could be used for relative humidity measurement. The proposed sensor showed a poor response towards the change in the relative humidity level below 56% RH. The flat response of SnO₂ based sensor in the range of below 60% RH was also reported in [12] and in [22] that was based on the field-effect transistor (FET) nanodevice because the pure SnO₂ did not show a significant change in the impedance until humidity reached as high as 60% RH, while a significant response was observed in the humidity level between 56% RH and 90% RH with the attenuation increasing from 2.9 dB to 56.9 dB. Due to the range limitation of the calibration hygrometer and homemade humidity box, the changes in the relative humidity from 0 to 20% RH and 90% RH to 100% RH were not measured.

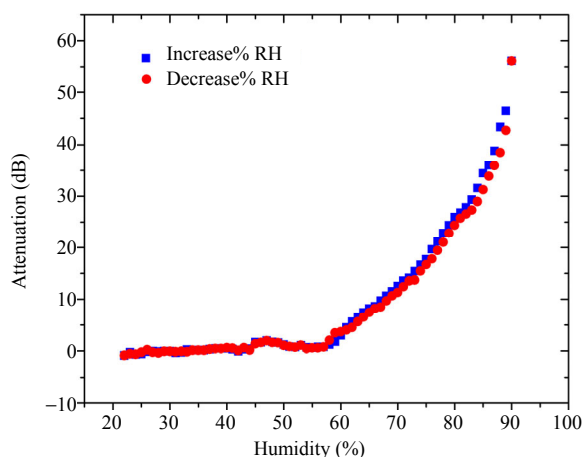


Fig. 5 Response to humidity occurs in the range of 56% RH to 90% RH.

Figure 6 shows the response of SnO₂ coated optical waveguide to changes in the relative humidity from ambient condition (~54% RH) to different values of higher relative humidity (%RH). It can be seen that the proposed sensor shows an excellent reversible response to changes in %RH. The sensitivity of the proposed sensor is calculated to be ~2 dB/% RH. The high sensitivity of the

proposed sensor is attributed to the nanosize of the SnO₂ nanoparticles (27.08 nm) used in this work. The smaller size of SnO₂ corresponds to the larger surface area, which increases water adsorption and results in a better sensitivity of the sensor [23]. Note that the response time in Fig. 6 is relatively longer compared with the other all-optical humidity sensors

[14, 16], which were limited by the relatively large humidity box [$50 \times 40 \times 12$ (cm³)] that was not hermetically sealed. The large box was used instead of small box to cover a pair of 5-axis fiber alignment stages. However, the large humidity box is not suitable for studying the response and recovery time because of the slow humidity adjustment rate.

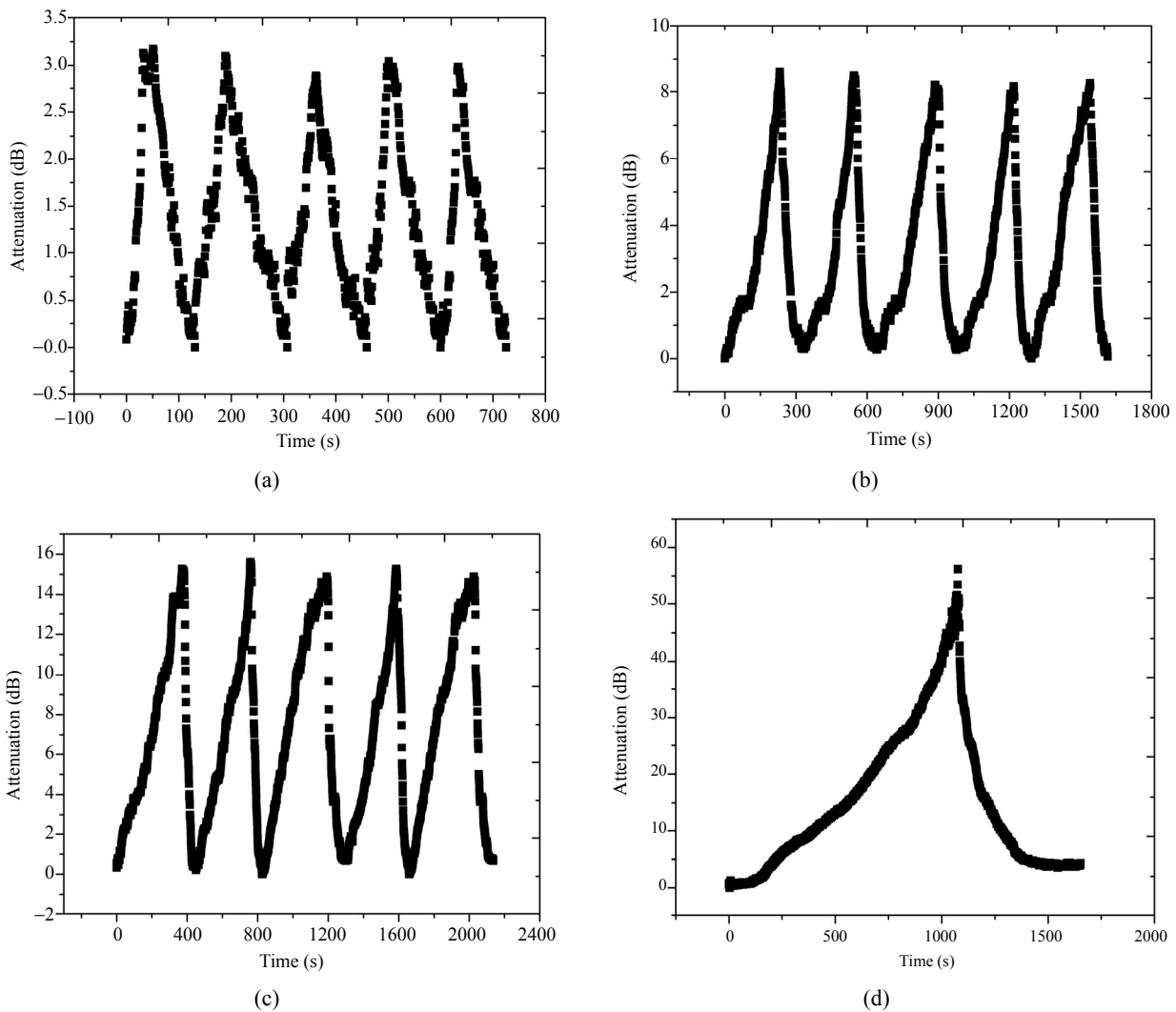


Fig. 6 Change in attenuation when humidity increases in the humidity-controlled box at (a) 63% RH, (b) 66% RH, (c) 70% RH, and (d) 90% RH.

In order to measure the response time of the proposed sensor itself, exhaling from a person (with near 100% RH measured by using a hygrometer) was introduced to the sensor in the ambient condition (54% RH). The result is shown in Figs. 7(a) and 7(b). The proposed sensor exhibited a fast response to the presence and absence of humid air

flow. From Fig. 7(b), the response time of less than 2.5 s and recovery time of less than 3.5 s were observed in the RH measurements. The response (increase) slope seemed to have a larger gradient than the recovery slope (decrease), and the similar response/recovery curves were also reported in other optical humidity sensors [15]. The response time

and recovery time of the proposed sensor were faster than that reported in [14] whose response time and recovery time were 3 s and 10 minutes, respectively. In addition, the recovery time was faster than

that of the fiber optic-based sensor [15]. The comparison of this work with previous all-optical sensor based SnO₂ nanoparticle is shown in Table 1.

Table 1 Comparison between this work and previous work in all-optical humidity sensor with based SnO₂ nanoparticles.

Parameter	Based planar optical waveguide [14]	Based optical fiber		This work
		[7]	[15]	
SnO ₂ location	Cladding of planar optical waveguide	End of the optical fiber	On the tapered fiber	Uppercladding of planar optical waveguide
SnO ₂ deposition	Screen printing	Electrospray pyrolysis	Sputtering	Drop coating
Thickness of SnO ₂	20 μm	Hundreds of nanometers	280 nm	2.27 μm
Width of SnO ₂	Length 4 mm	Diameter 125 μm	Length 4.2 mm	Diameter 1.4 mm
Response time	3 s	-	1.5 s	2.5 s
Recovery time	10 min	-	4 s	3.5 s
Range of humidity measurement	3% RH – 98% RH	2% RH – 40 % RH	20% RH – 90% RH	56% RH – 90% RH

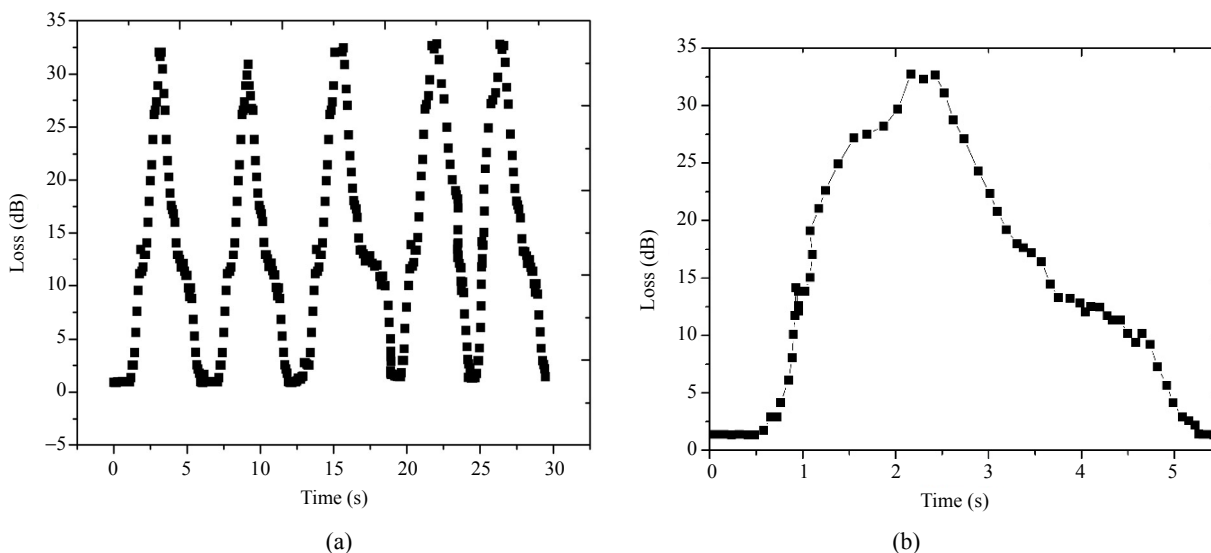


Fig. 7 Response time of the proposed sensor: (a) periodic response/recovery curves of the proposed sensor exposed to nearly 100% RH from ambient humidity (54% RH) and (b) a single response/recovery curves.

3.3 Analysis of humidity sensing ability

To ascertain the polarization dependency of light transmission through the SnO₂ coated waveguide, the polarization dependent loss was measured. The optical polarization state of light incident upon the SnO₂ coated waveguide was changed by adjusting the polarization controller, and the polarization states of light at the waveguide output was measured by using a polarimeter (Thorlabs PAX 5710). The result is shown in Fig. 8. It can be seen that SnO₂

film does not have significant polarization selection characteristics at different laser pump powers or wavelengths, which means that the response of the proposed sensor to relative humidity change is not polarization dependent.

By analyzing the results obtained, a model of water adsorption mechanism in the SnO₂ layer is proposed and shown in Fig. 9. Figures 9(a) and 9(b) show photos of the SnO₂ coating on the proposed waveguide at ambient humidity (~54% RH) and humid air (~100% RH), respectively. A few water

droplets indicated by bright spots can be seen on the surface of the SnO_2 coating. When humid air from person exhaling was introduced, these spots became more apparent and appeared to be joining up because water droplet in the SnO_2 layer surface was reflecting the camera light [24]. We believe that this indicates water permeation into the SnO_2 film, which reduced the beam confinement in the waveguide and resulted in an increase in the light transmission loss. Figure 9(c) shows the water adsorption mechanism of our proposed model. At lower humidity ($< 56\% \text{RH}$), the water vapors only adhered onto the surface of the SnO_2 layer. At intermediate humidity ($56\% \text{RH} - 86\% \text{RH}$), a small amount of water penetrated into the SnO_2 layer, which caused a small radiation loss and affected the transverse guiding of light in the cladding. Meanwhile, at higher humidity ($> 86\% \text{RH}$), water was adsorbed in huge amount into the volume of the film, therefore causing a significant radiation loss. This mechanism helps to explain the observation in Fig. 5, which have 3 slopes: (a) slope below $56\% \text{RH}$ that indicates the surface adsorption of water by the SnO_2 layer, (b) slope between $56\% \text{RH}$ and $86\% \text{RH}$ that indicates the increasing adsorption of water by the SnO_2 layer, and (c) slope above $86\% \text{RH}$ that indicates near saturated adsorption of water by the SnO_2 layer. The proposed sensor's insensitivity to relative humidity lower than $56\% \text{RH}$ might be caused by the thickness of the film which resulted in a very small water adsorption level which could not affect the light confinement in the waveguide core significantly.

The ability to introduce SnO_2 coating by using the drop coated method provides a simple and effective means for humidity sensor fabrication. The proposed sensor can operate in the humidity range from $56\% \text{RH}$ to $90\% \text{RH}$. This relative humidity range is widely used in agricultural and biological applications, such as feeding room, greenhouse, and proving room [25].

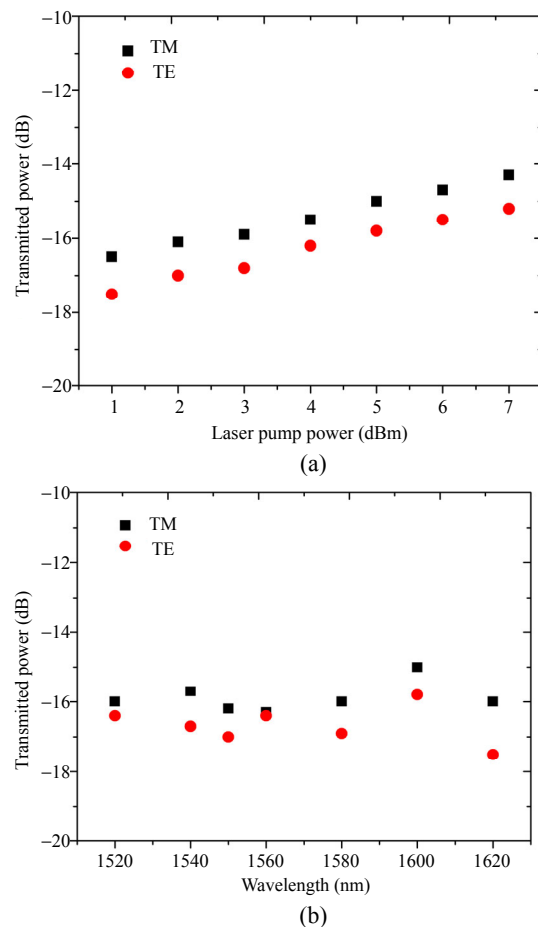


Fig. 8 Response of transmitted power to TE and TM polarizations for different pump powers (a) and wavelengths (b).

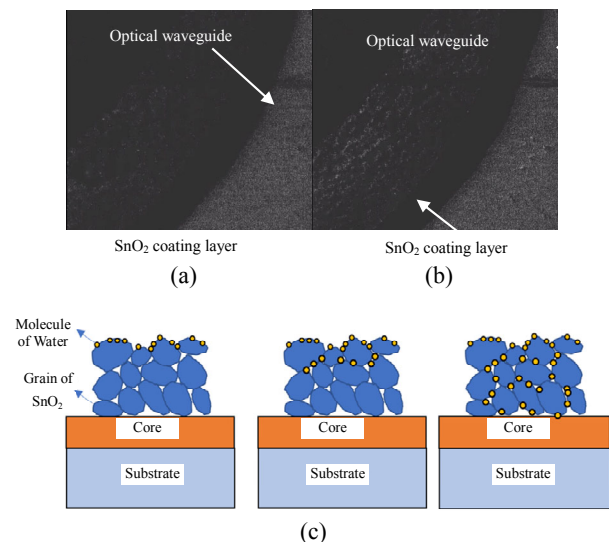


Fig. 9 Absorption phenomenon in different conditions of humidity: (a) before humid air was introduced in the ambient environment, (b) when humid air from exhaling was introduced, and (c) schematic of water absorptions at low humidity, intermediate humidity, and large humidity.

3.4 Comparison with another all-optical humidity sensor

Many works have also been reported on optical humidity sensor based on optical fiber with various structures, such as side-polished/D-shaped [26], tapered [27], and U-bend [28]. The fastest response time reported to date was achieved by using a U-bend microfiber (3 ms) [3]. However, since the uses of these fibers require the removal of the fiber cladding, the mechanical strength of the fibers is compromised [29]. In addition, this fabrication process is also relatively time consuming [30].

The planar waveguide, on the other hand, is relatively strong. The waveguide core can be exposed by using a standard etching process used in the established semiconductor manufacturing industry. In terms of mass production, the planar waveguide-based sensor is much more attractive than their optical fiber counterparts because it allows mounting of miniature integrated optical circuits

onto a single substrate platform [31]. In addition, accurately localized deposition of SnO₂ drop coatings can be achieved in mass production by use of an automated micropipette positioning and dispensing system.

In terms of the sensing material, various sensing materials such as Ag-polyaniline [32], graphene oxide [18], reduced graphene oxide [33], and titanium oxide [34], have been used on the planar optical waveguide. A comparison of their performances is summarized in Table 2. It can be seen that the sensitivity of the proposed sensor is higher than that of another sensor, but the measurement range and response time are still to be improved. This can be achieved with the removal of the coffee ring effect by using the ion doping like KCl [12] or Ag [35], composited with graphene oxide [36–38], MoS₂ [39], or TiO₂ [40] to achieve a broader measurement range and a shorter response time.

Table 2 Comparison between various materials of planar optical waveguide as humidity sensor for interval 2008–2018.

Reference	Year	Sensing material	Range	Sensitivity	Response time
[32]	2008	Ag-polyaniline	20% RH–92% RH	35.6 mV/% RH	8 s
[18]	2014	Graphene oxide (GO)	60% RH–100% RH	0.553 dB/% RH	~1 s
[33]	2016	Reduced-GO	35% RH–95% RH	0.22 dB/% RH	0.68 s
[34]	2016	TiO ₂	35% RH–95% RH	0.21 dB/% RH	0.72 s
ThisWork	2018	SnO ₂	56% RH–90% RH	2 dB/% RH	2.5 s

4. Conclusions

The humidity sensing ability of a SnO₂-coated planar optical waveguide by the simple multiple drop coating method has been studied. The loss of the proposed sensor is found to be affected by the relative humidity of its surroundings. A decrease in the transmitted power at higher humidity is due to water adsorption that radiates light from the core. The proposed sensor exhibits a fast response of less than 2.5 s to humid air. In addition, it shows a good sensitivity of ~2 dB/% RH in the humidity range from 56% RH to 90% RH with a very good

repeatability. The proposed sensor has a potential application in the long distance and remote agricultural and biological humidity sensing.

Acknowledgment

This work is partially supported by the Ministry of Research, Technology & Higher Education of Indonesia with PMDSU scholarship funding, and the Malaysia Ministry of Higher Education (MOHE) (LRGS(2015)/NGOD/UM/KPT). We thank Gan and Wensin for assistance during the humidity measurement preparation and waveguide fabrication.

Open Access This article is distributed under the terms of the Creative Commons Attribution 4.0 International License (<http://creativecommons.org/licenses/by/4.0/>), which permits unrestricted use, distribution, and reproduction in any medium, provided you give appropriate credit to the original author(s) and the source, provide a link to the Creative Commons license, and indicate if changes were made.

References

- [1] Y. Kuwahara, S. Tamagawa, T. Fujitani, and H. Yamashita, "Removal of phosphate from aqueous solution using layered double hydroxide prepared from waste iron-making slag," *Bulletin of the Chemical Society of Japan*, 2016, 89(4): 472–480.
- [2] J. Jiang, W. Zhou, Y. Gao, L. Wang, F. Wang, H. Chu, *et al.*, "Feasibility of manufacturing ultra-high performance cement-based composites (UHPCs) with recycled sand: a preliminary study," *Waste Management*, 2019, 83: 104–112.
- [3] G. Y. Chen, X. Wu, Y. Q. Kang, L. Yu, T. M. Monro, D. G. Lancaster, *et al.*, "Ultra-fast hygrometer based on U-shaped optical microfiber with nanoporous polyelectrolyte coating," *Scientific Reports*, 2017, 7(1): 1–7.
- [4] S. Borini, R. White, D. Wei, M. Astley, S. Haque, E. Spigone, *et al.*, "Ultrafast graphene oxide humidity sensors," *ACS Nano*, 2013, 7(12): 11166–11173.
- [5] W. Xuan, M. He, N. Meng, X. He, W. Wang, J. Chen, *et al.*, "Fast response and high sensitivity ZnO/glass surface acoustic wave humidity sensors using graphene oxide sensing layer," *Scientific Reports*, 2014, 4: 7206.
- [6] Y. Peng, Y. Zhao, M. Q. Chen, and F. Xia, "Research advances in microfiber humidity sensors," *Small*, 2018, 14(29): 1800524.
- [7] M. Consales, A. Buosciolo, A. Cutolo, G. Breglio, A. Irace, S. Buontempo, *et al.*, "Fiber optic humidity sensors for high-energy physics applications at CERN," *Sensors and Actuators B: Chemical*, 2011, 159(1): 66–74.
- [8] D. Zhang, X. Zong, Z. Wu, and Y. Zhang, "Ultrahigh-performance impedance humidity sensor based on layer-by-layer self-assembled tin disulfide/titanium dioxide nanohybrid film," *Sensors and Actuators B: Chemical*, 2018, 266: 52–62.
- [9] D. Zhang, H. Chen, P. Li, D. Wang, and Z. Yang, "Humidity sensing properties of metal organic framework-derived hollow ball-like TiO₂ coated QCM sensor," *IEEE Sensors Journal*, 2019, 19(8): 2909–2915.
- [10] D. Zhang, H. Chang, P. Li, R. Liu, and Q. Xue, "Fabrication and characterization of an ultrasensitive humidity sensor based on metal oxide/graphene hybrid nanocomposite," *Sensors and Actuators B: Chemical*, 2016, 225: 233–240.
- [11] D. Zhang, D. Wang, X. Zong, G. Dong, and Y. Zhang, "High-performance QCM humidity sensor based on graphene oxide/tin oxide/polyaniline ternary nanocomposite prepared by in-situ oxidative polymerization method," *Sensors and Actuators B: Chemical*, 2018, 262: 531–541.
- [12] X. Song, Q. Qi, T. Zhang, and C. Wang, "A humidity sensor based on KCl-doped SnO₂ nanofibers," *Sensors and Actuators B: Chemical*, 2009, 138(1): 368–373.
- [13] Q. Kuang, C. Lao, Z. L. Wang, Z. Xie, and L. Zheng, "High-sensitivity humidity sensor based on a single SnO₂ nanowire," *Journal of the American Chemical Society*, 2007, 129(19): 6070–6071.
- [14] Z. A. Ansari, R. N. Karekar, and R. C. Aiyer, "Humidity sensor using planar optical waveguides with claddings of various oxide materials," *Thin Solid Films*, 1997, 305(1–2): 330–335.
- [15] J. Ascorbe, J. M. Corres, I. R. Matias, and F. J. Arregui, "High sensitivity humidity sensor based on cladding-etched optical fiber and lossy mode resonances," *Sensors and Actuators B: Chemical*, 2016, 233: 7–16.
- [16] W. H. Lim, Y. K. Yap, W. Y. Chong, and H. Ahmad, "All-optical graphene oxide humidity sensors," *Sensors*, 2014, 14(12): 24329–24337.
- [17] Z. Harith, N. Irawati, M. Batumalay, H. A. Rafaie, G. Yun, S. W. Harun, *et al.*, "Relative humidity sensor employing optical fibers coated with ZnO nanostructures," *Indian Journal of Science and Technology*, 2015, 8(35): 0974–6846.
- [18] L. Bo, P. Wang, Y. Semenova, and G. Farrell, "Optical microfiber coupler based humidity sensor with a polyethylene oxide coating," *Microwave and Optical Technology Letters*, 2015, 57(2): 457–460.
- [19] N. Irawati, H. A. Rahman, H. Ahmad, and S. W. Harun, "A PMMA microfiber loop resonator based humidity sensor with ZnO nanorods coating," *Measurement*, 2017, 99: 128–133.
- [20] S. Zhan, D. Li, S. Liang, X. Chen, and X. Li, "A novel flexible room temperature ethanol gas sensor based on SnO₂ doped polydiallyldimethylammonium chloride," *Sensors*, 2013, 13(4): 4378–4389.
- [21] A. Asnawi, G. Yudoyono, and Y. H. Pramono, "Fabrication of straight optical waveguides based on SnO₂ nanomaterials," *Universal Journal of Physics and Application*, 2017, 11(4): 135–138.
- [22] D. Zhang, H. Chang, and R. Liu, "Humidity-sensing properties of one-step hydrothermally synthesized tin dioxide-decorated graphene nanocomposite on polyimide substrate," *Journal of Electronic Materials*, 2016, 45(8): 4275–4281.
- [23] G. J. Li, X. H. Zhang, and S. Kawi, "Relationships

- between sensitivity, catalytic activity, and surface areas of SnO₂ gas sensors,” *Sensors and Actuators B: Chemical*, 1999, 60(1): 64–70.
- [24] S. K. Nayar and S. G. Narasimhan, “Vision in bad weather,” in *Proceedings of the Seventh IEEE International Conference on Computer Vision*, Kerkyra, Greece, 1999, pp. 820–827.
- [25] R. Gao, D. F. Lu, J. Cheng, Y. Jiang, L. Jiang, and Z. M. Qi, “Humidity sensor based on power leakage at resonance wavelengths of a hollow core fiber coated with reduced graphene oxide,” *Sensors and Actuators B: Chemical*, 2016, 222: 618–624.
- [26] A. Alvarez-Herrero, H. Guerrero, and D. Levy, “High-sensitivity sensor of low relative humidity based on overlay on side-polished fibers,” *IEEE Sensors Journal*, 2004, 4(1): 52–56.
- [27] C. Bariáin, I. R. Matías, F. J. Arregui, and M. López-Amo, “Optical fiber humidity sensor based on a tapered fiber coated with agarose gel,” *Sensors and Actuators B: Chemical*, 2000, 69(1–2): 127–131.
- [28] B. D. Gupta, “A novel probe for a fiber optic humidity sensor,” *Sensors and Actuators B: Chemical*, 2001, 80(2): 132–135.
- [29] D. C. Bownass, J. S. Barton, and J. D. Jones, “Serially multiplexed point sensor for the detection of high humidity in passive optical networks,” *Optics Letters*, 1997, 22(5): 346–348.
- [30] J. Ascorbe, J. M. Corres, F. J. Arregui, and I. R. Matías, “Recent developments in fiber optics humidity sensors,” *Sensors*, 2017, 17(4): 1–23.
- [31] K. R. Kribich, R. Copperwhite, H. Barry, B. Kolodziejczyk, J. M. Sabattié, K. O’Dwyer, *et al.*, “Novel chemical sensor/biosensor platform based on optical multimode interference (MMI) couplers,” *Sensors and Actuators B: Chemical*, 2005, 107(1): 188–192.
- [32] M. V. Fuke, A. Vijayan, P. Kaniatkar, M. Kulkarni, B. B. Kale, and R. C. Aiyer, “Ag-polyaniline nanocomposite cladded planar optical waveguide based humidity sensor,” *Journal of Materials Science: Materials in Electronics*, 2009, 20(8): 695–703.
- [33] M. Ghadiry, M. Gholami, C. K. Lai, H. Ahmad, and W. Y. Chong, “Ultra-sensitive humidity sensor based on optical properties of graphene oxide and nano-anatase TiO₂,” *PLoS One*, 2016, 11(4):1–14.
- [34] M. Ghadiry, M. Gholami, L. C. Kong, C. W. Yi, H. Ahmad, and Y. Alias, “Nano-anatase TiO₂ for high performance optical humidity sensing on chip,” *Sensors*, 2015, 16(1): 39.
- [35] V. K. Tomer and S. Duhan, “A facile nanocasting synthesis of mesoporous Ag-doped SnO₂ nanostructures with enhanced humidity sensing performance,” *Sensors and Actuators B: Chemical*, 2016, 223: 750–760.
- [36] H. Zhang, J. Feng, T. Fei, S. Liu, and T. Zhang, “SnO₂ nanoparticles-reduced graphene oxide nanocomposites for NO₂ sensing at low operating temperature,” *Sensors and Actuators B: Chemical*, 2014, 190: 472–478.
- [37] D. Zhang, J. Tong, and B. Xia, “Humidity-sensing properties of chemically reduced graphene oxide/polymer nanocomposite film sensor based on layer-by-layer nano self-assembly,” *Sensors and Actuators B: Chemical*, 2014, 197: 66–72.
- [38] D. Zhang, J. Tong, B. Xia, and Q. Xue, “Ultra-high performance humidity sensor based on layer-by-layer self-assembly of graphene oxide/polyelectrolyte nanocomposite film,” *Sensors and Actuators B: Chemical*, 2014, 203: 263–270.
- [39] D. Zhang, Y. Sun, P. Li, and Y. Zhang, “Facile fabrication of MoS₂-modified SnO₂ hybrid nanocomposite for ultrasensitive humidity sensing,” *ACS Applied Materials & Interfaces*, 2016, 8(22): 14142–14149.
- [40] W. P. Tai and J. H. Oh, “Fabrication and humidity sensing properties of nanostructured TiO₂ SnO₂ thin films,” *Sensors and Actuators B: Chemical*, 2002, 85(1–2): 154–157.